Supporting Information

Morphological and Crystalline Evolution of Nanostructured MnO_2 and Their Application in Lithium-Air Batteries

Tu T. Truong,[†] Yuzi Liu,[†] Yang Ren,[‡] Lynn Trahey,[§] and Yugang Sun [†,]*

[†]Center for Nanoscale Materials, Argonne National Laboratory, 9700 South Cass Avenue, Argonne, Illinois, 60439, USA

[‡]X-ray Science Division, Advanced Photo Source, Argonne National Laboratory, 9700 South Cass Avenue, Argonne, Illinois, 60439, USA

[§]Chemical Sciences and Engineering Division, Argonne National Laboratory, 9700 South Cass Avenue, Argonne, Illinois, 60439, USA

[*]Author to whom correspondence should be addressed. E-mail: ygsun@anl.gov

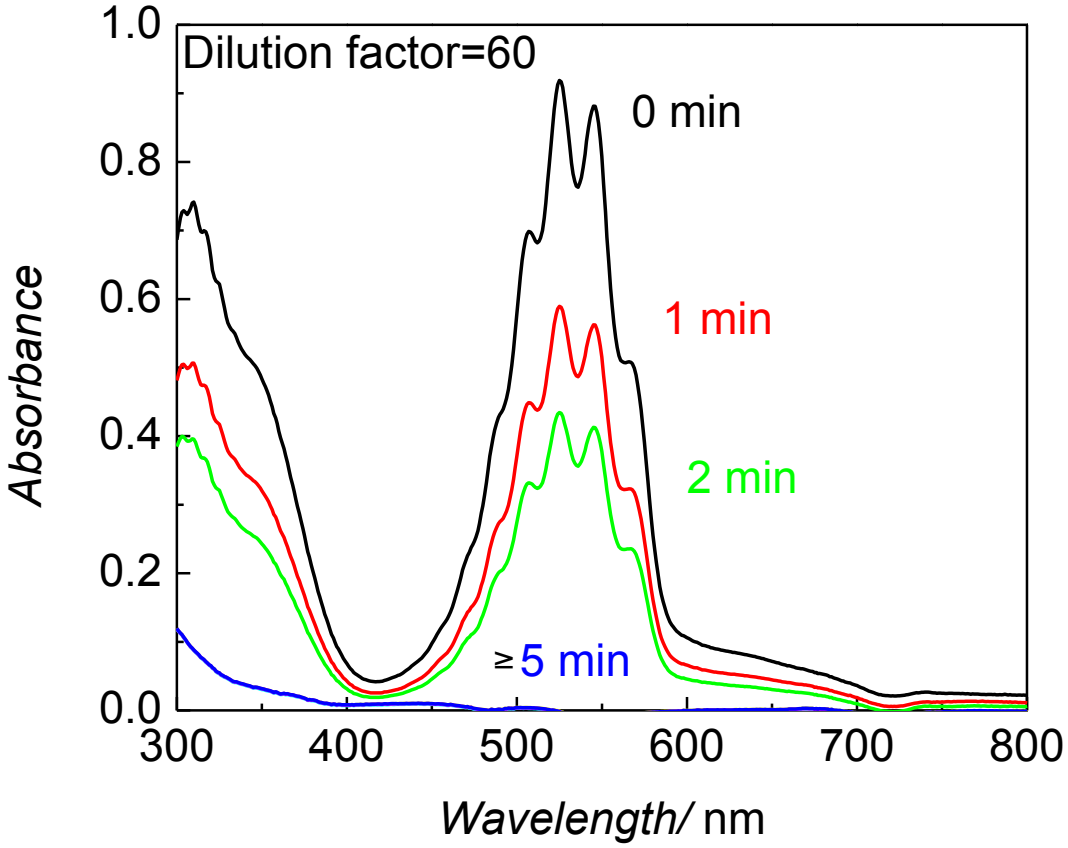

Figure S1. Absorption spectra of reaction solutions at different reaction times. The MnO_2 powders were removed through centrifuge before the spectra were taken.

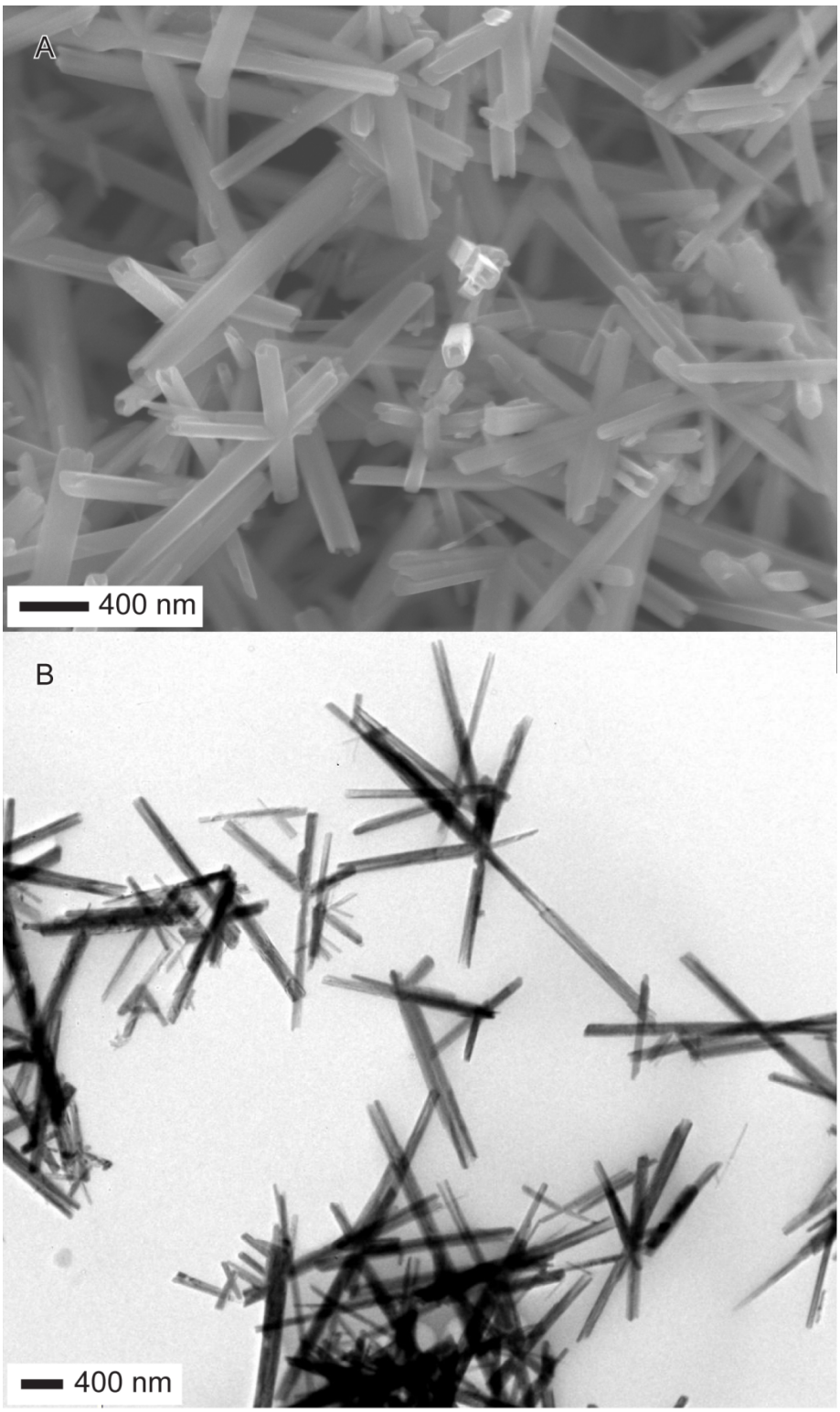

Figure S2. Typical (A) SEM and (B) TEM images of the product formed at 6 h as shown in Fig. 1F, clearly highlighting the abundance of uniform hollow nanotubes.

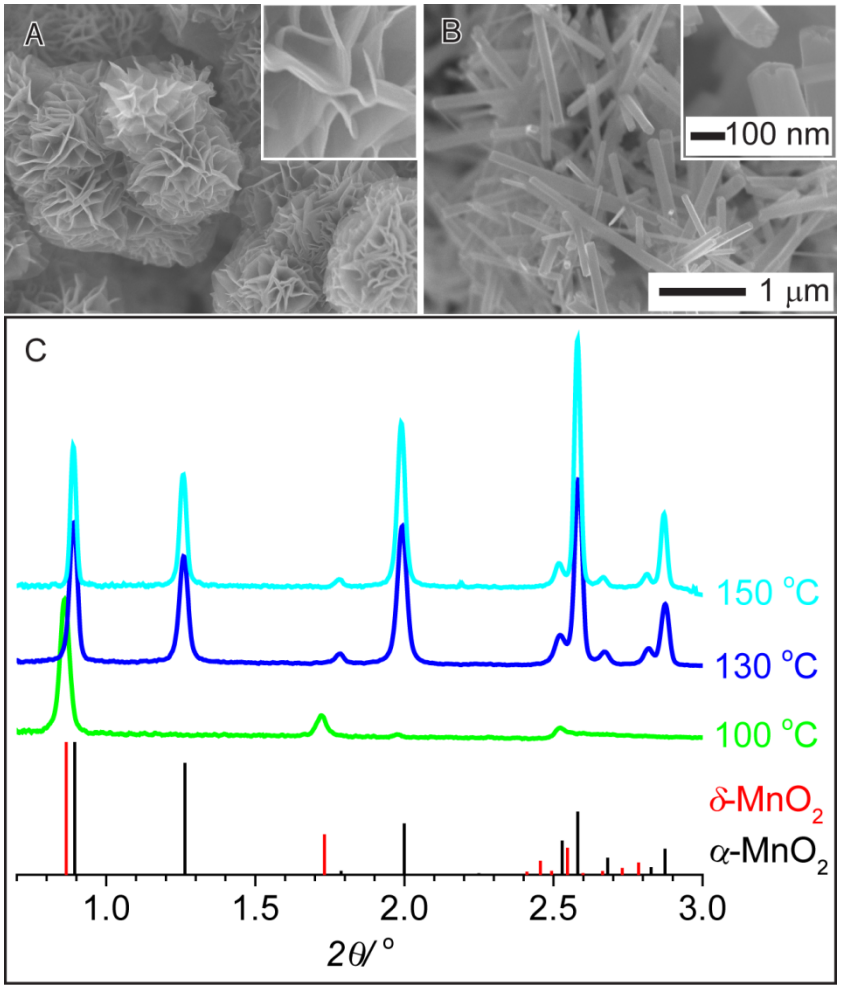

Figure S3. Influence of reaction temperature on the MnO_2 nanostructures. (A, B) SEM images of the MnO_2 nanostructured obtained at different temperatures: (A) 100 and (B) 130 ^{o}C. (C) XRD patterns of the MnO_2 nanostructures obtained at different temperatures.

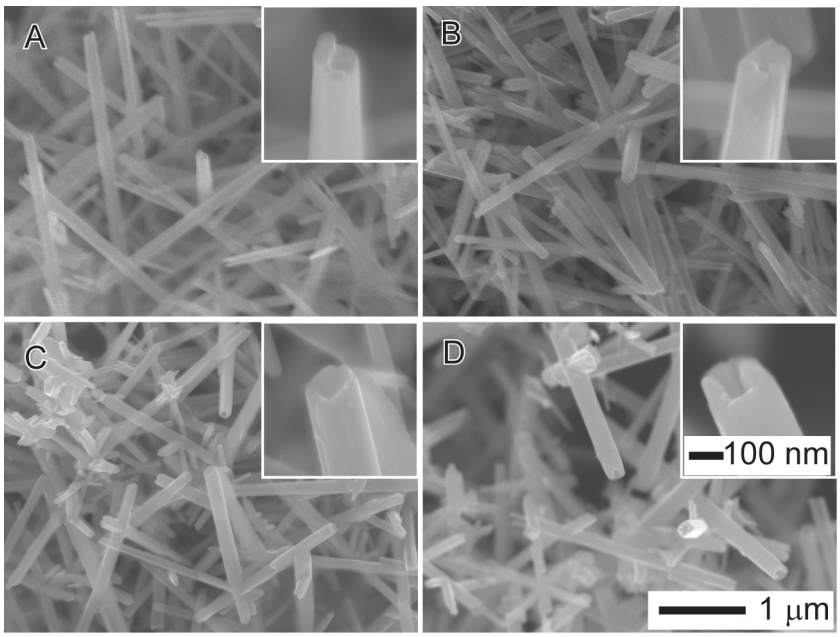

Figure S4. Influence of pressure on the MnO_2 nanostructures. SEM images of the MnO_2 nanotubes obtained under different atmosphere pressures: (A) 58, (B) 60, (C) 62, and (D) 80 psi.

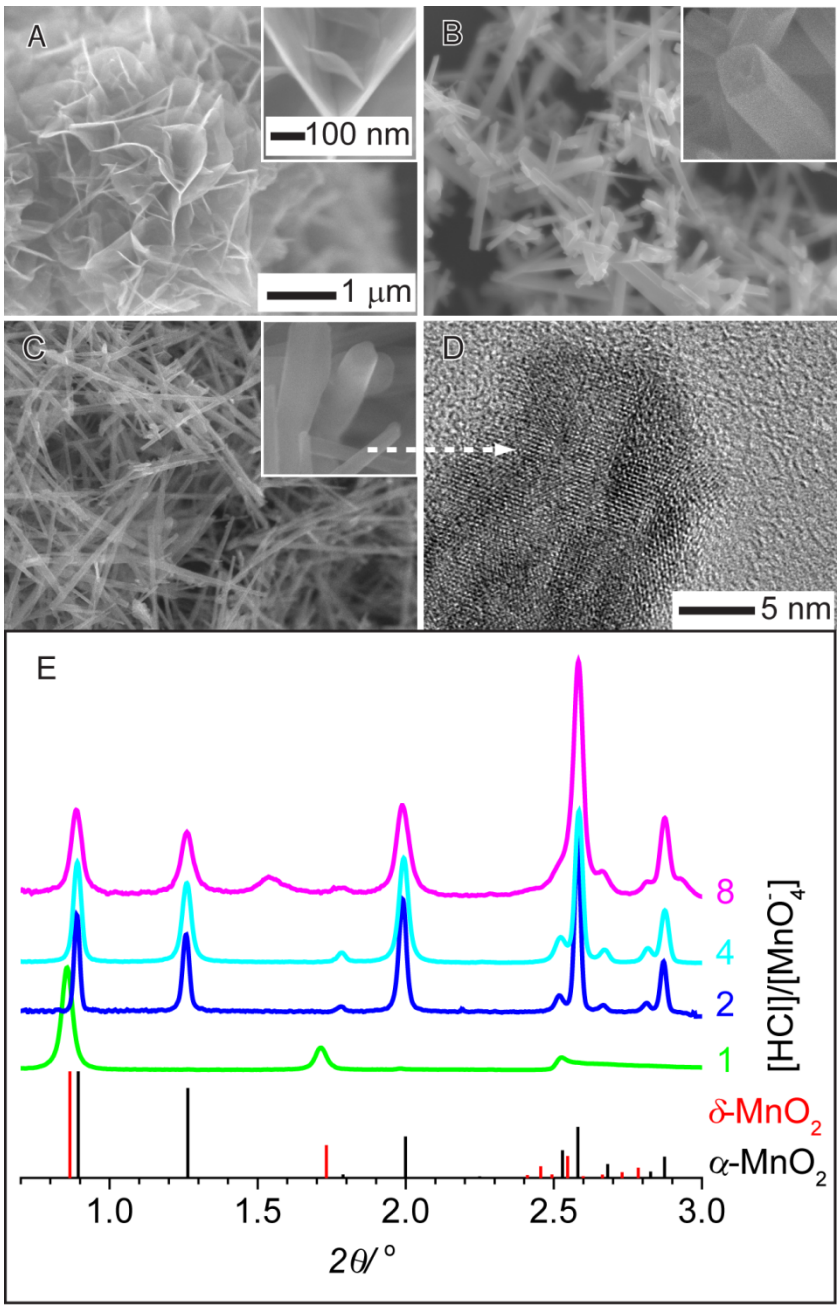

Figure S5. Influence of the concentration of HCl on the MnO_2 nanostructures. (A-C) SEM images of the MnO_2 nanostructures synthesized at different ratios of $[HCl]/[KMnO_4]$: (A) 1, (B) 2, and (C) 8. (D) High resolution TEM image of a nanowire synthesized at $[HCl]/[KMnO_4] = 8$. (E) XRD patterns of the synthesized MnO_2 nanostructures shown in (A-C).

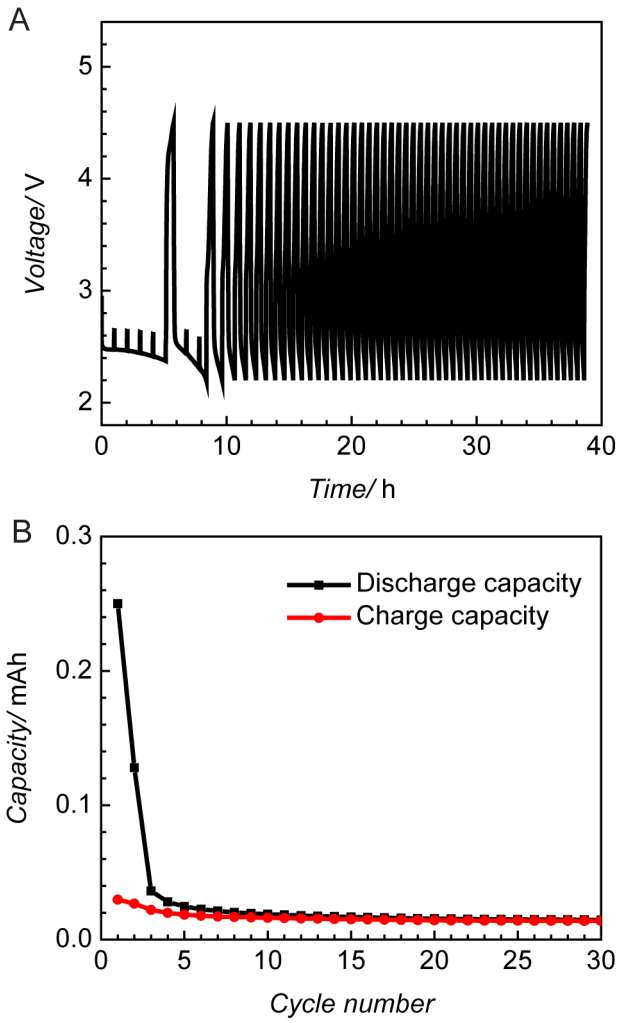

Figure S6. Electrochemical characterization of a lithium-air battery cell using an air cathode without MnO_2 nanostructures. (A) Recorded voltage as a function of time during multiple discharge/charge cycles. (B) Variation of the discharge and charge capacity against the cycle number.

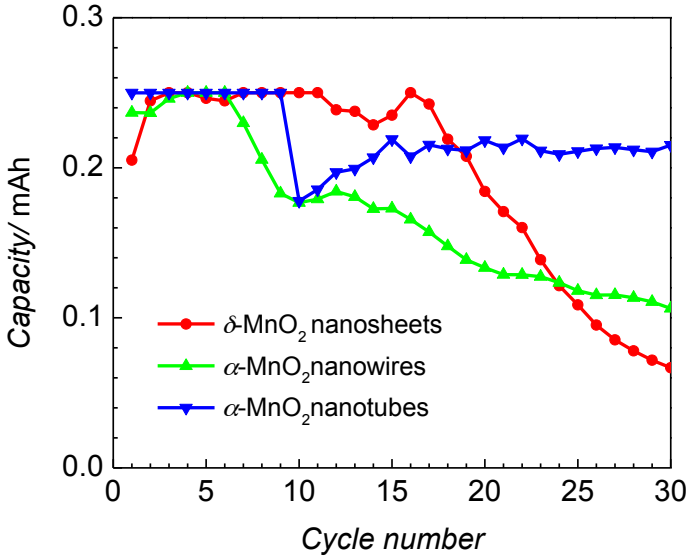

Figure S7. Variation of the charge capacity against the cycle number for different lithium-air cells as shown in Figure 7.

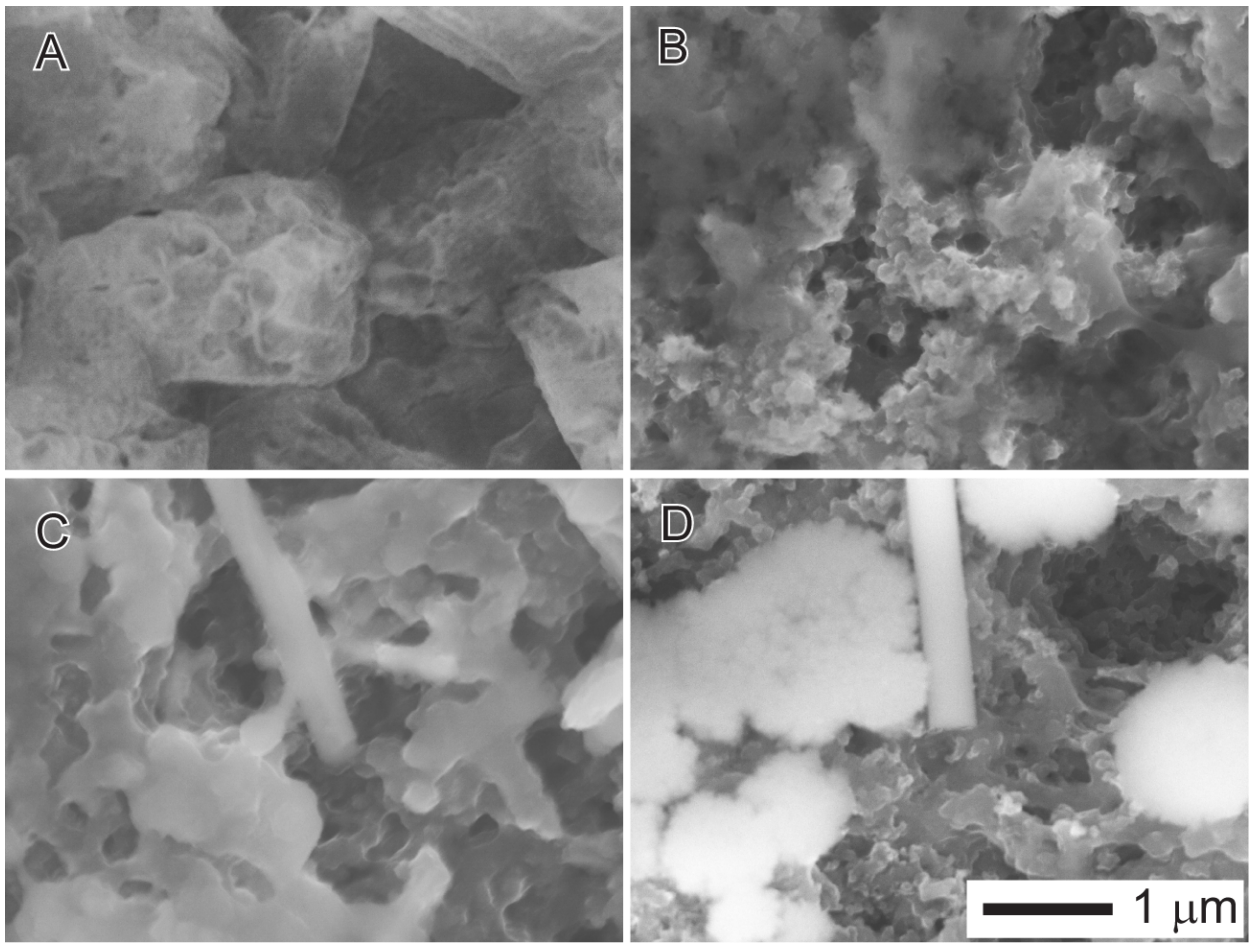

Figure S8. SEM images of the cathode electrodes after the corresponding lithium-oxygen cells had been cycled for 30 cycles and completely discharged. The electrode shown in (A) did not include MnO_2 nanostructures. The electrodes shown in (B-D) included (B) δ-MnO_2 nanosheets, (C) α-MnO_2 nanowires, and (D) α-MnO_2 nanotubes.